5th ECPMG Delft · 2024

Proceedings of the 5th ECPMG 2024
5th European Conference on Physical Modelling in Geotechnics
2-4 October 2024, Delft, the Netherlands

Centrifuge modelling of a river embankment slope failure induced by a high-water event

E. Dodaro, M. Marcolongo, G. Gottardi
University of Bologna, Department of Civil, Chemical, Environmental and Materials Engineering, Bologna, Italy, elena.dodaro2@unibo.it, mario.marcolongo@unibo.it, guido.gottardi2@unibo.it

C.G. Gragnano
Laboratoire Navier, Ecole des Ponts ParisTech, Gustave Eiffel University, CNRS, Marne-la-Vallée, France, carmine-gerardo.gragnano@enpc.fr

A. Bassi
Interregional Agency for the Po River, AIPO, Italy, agnese.bassi@agenziapo.it

S.A. Stanier, G.M.B. Viggiani
Cambridge University, Engineering Department, Cambridge, United Kingdom, sas229@cam.ac.uk, gv278@cam.ac.uk

ABSTRACT: River floods rank among the most significant natural hazard in Europe, causing substantial economic and human losses and are frequently due to severe damages endured by water retaining earthworks, under extreme weather events. In this framework, a reliable assessment of the existing river embankments safety conditions, represents a key aspect to enhance the resilience of these critical infrastructures. This paper presents the model preparation technique, experimental setup and preliminary findings of a centrifuge test conducted on a river embankment model, subjected to a simulated high-water event. The earthfill was constructed with natural silty sand, sampled along a floodplain area of Secchia river, a tributary of the main Po River in Italy, where a recent breach occurred. To investigate the hydro-mechanical behaviour and the potential failure mechanisms of the earth structure, induced by the progressive raising of the water table, in-house built miniaturized tensiometers, pore pressure transducers, a high-resolution camera and a displacement sensor have been used. The study aims to shed light on the effect of time-dependent hydraulic loadings on the river embankment stability and to support the development of more reliable flood risk reduction strategies.

1 INTRODUCTION

As consequence of the significant impact of climate change and spatial expansion of urbanized areas, extreme geohazard events, resulting from natural, active geological processes are becoming more frequent and of greater magnitude and consequence. Forecasting models suggest that climate change will be a determining factor in intensifying the hydrological cycle, with far-reaching impacts on runoff regimes of streams and watercourses, thus significantly reducing the return times of droughts and flood events (Alcamo et al. 2007). This means that existing water retaining infrastructures, such as earthen river embankments, are expected to withstand extreme stresses, being subjected to hydraulic loading hardly experienced in the past, in terms of duration and intensity. In this context, the need for strengthening and enhancing the resilience of these critical infrastructures, through the profound knowledge of the pressures acting on them and a reliable stability assessment, represents a pivotal aspect. Addressing this task requires the estimation of the actual pore water pressure distribution within the earthfill and acknowledging the role of river stage fluctuations on the groundwater seepage process. Insights into the evolution of the hydraulic regime within a river embankment section during a high-water event can be obtained from on-site monitoring activities (Rocchi et al., 2018), although they are characterized by significant uncertainties, or through physical modelling in highly controlled environments, such as geotechnical centrifuges (Cargill and Ko, 1983; Singh et al., 2019; Ventini et al., 2023). This paper briefly presents the experimental setup and preliminary outcomes of a centrifuge test carried out as part of the EU GEOLAB - RES FLUCTIS (*Assessing River Embankments Stability to FLoods through*

Unsaturated Centrifuge Testing In transient Seepage conditions) project. The experimental investigation was conducted on a natural silty sand river embankment model, compacted in unsaturated conditions and subjected to a simulated flood event. The embankment was founded on a fully saturated Speswhite kaolin layer and thoroughly instrumented, to monitor pore water pressure changes and deformations. The aim of the test is to investigate the effect of a high-water event on the hydraulic characteristics of the embankment model and to study the triggering and development of a typical failure mechanism, i.e. the macro-instability of the landside slope. The main cause behind this failure is the seepage within the embankment body, leading to the development of high pore water pressures and to the subsequent decrease in the effective shear strength of the soil (Van et al., 2022).

2 CENTRIFUGE TEST AND MODEL FEATURES

2.1 Materials and sample preparation

The experiment was carried out at the Schofield Centre of the University of Cambridge (UK), on the 150 g-ton Turner beam centrifuge, with a nominal radius of 4.125 m and a payload of 1000 kg (Madabhushi, 2015). A target acceleration of 50 g was gradually applied to the overall centre of the mass, located at 4.08 m from the centre of rotation, close to the embankment base. Thus an average geometric scaling factor N = 50 can be reasonably assumed for the whole earth structure. A comprehensive set of scaling laws relating the model to the prototype response can be found in Garnier et al. (2007).

The small-scale physical model was prepared within a prismatic strongbox, whose internal dimensions are: length = 790 mm, height = 475 mm, width = 180 mm, with a front wall made of transparent Perspex, allowing for the analysis of the real-time pictures captured during the test.

A typical embankment section of the Alpine and Apennine riverbank systems of the main river Po (Northern Italy), which have recently experienced multiple overall collapses and breaches, due to high-water events, has been taken as reference in the present study. The filling material is prevalently constituted by a heterogeneous mixture of sands and silt, while the subsoil frequently consists of clayey or silty deposits. Similarly, the soil selected for the embankment model is a natural silty sand, sampled from a floodplain area of the Secchia river (Soliera, province of Modena, Italy), while for the subsoil, a homogeneous consolidated layer of Speswhite kaolin has been used. The grain size distribution of the testing soils is shown in Fig. 1, while Table 1 lists the main physical and hydro-mechanical properties of the embankment body and foundation unit in the model condition. The parameters reported for the kaolin are those quoted by Viggiani (1992).

To obtain adequate shear strength characteristics and to reduce the hydraulic conductivity, the model embankment has been compacted within the strongbox into four layers, with the moist tamping technique, at a moisture content of 9.9 %, and at a dry density of 16.5 kN/m^3, representative for site conditions. Afterwards the embankment was manually shaped, using the edges of a trapezoidal acrylic template as a guide.

Table 1. Geotechnical properties of the embankment and foundation units in the model conditions.

Soil		**Silty sand**	**Speswhite kaolin**
Specific unit weight, G_s	-	2.69	2.61
Liquid limit, LL	(%)	23.04	58.00
Plastic limit, PL	(%)	19.30	34.00
Plasticity index, PI	(%)	3.74	24.00
Dry unit weight, γ_d	kN/ m^3	16.50	13.47
Water content, w	%	9.9	22.5
Initial suction, s	kPa	9.0	-
Hydraulic conductivity, k_{sat}	m/s	5.48E-07	-
Slope of normal consolidation line, λ	-	0.007	0.14
Slope of an unload-reload line, κ	-	0.011	0.03
Peak friction angle, φ'_p	°	37	-

To prepare the model foundation, Speswhite kaolin powder was mixed with water under vacuum to obtain a slurry with a water content approximately twice the liquid limit (LL). The slurry was poured into the strongbox and placed under a hydraulic press for the consolidation, to a maximum effective stress of about 850 kPa. At the end of the process, the sample was unloaded, and the clay layer was trimmed to a thickness of 100 mm.

To prevent the generation of preferential flow channels at the interface between the model and the strongbox and to ensure plane strain conditions for the earth structure, silicon grease was spread on the container walls and a glass clear silicon sheet was placed between the model and the container walls.

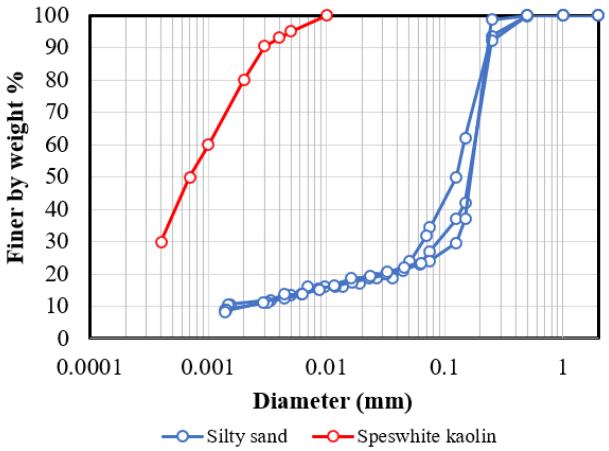

Figure 1. Grain size distributions of the testing soils.

2.2 Geometry and instrumentation

The silty sand embankment model was 150 mm high (7.5 m at the prototype scale) with an inclination for the riverside and landside slope of 1V:1H and 1.5V:1H, respectively (see Fig. 2). The adoption of such a steep slope for the landside, with a gradient that exceeds the effective friction angle, rarely encountered in reality, aims to promote the triggering of a peculiar failure mechanism, i.e. the macro instability of the landside, as a result of a progressive increase in saturation levels of the structure. Crest and base were 60 mm and 310 mm wide, respectively (3 m and 15.5 m at the prototype scale). The water retaining structure overlaid a 100 mm deep fine-grained layer (5 m at the prototype scale).

The embankment body was instrumented with four miniaturised tensiometers (labelled as T05, T06, T07, T08, in Fig. 2), characterized by a diameter of 9 mm and capable of measuring suctions up to -250 kPa and also suitable in the positive range. An additional pore water pressure transducer (PPT1) was installed at the base layer.

To monitor the vertical settlement of the earth structure, a linear variable displacement transducer (LVDT1) was placed on the crest of the earthwork, on the landward side. In addition, a pore water pressure transducer (PPT2), embedded in the foundation layer on the riverside, under a sand column, was used to monitor water level changes during the test. A Raspberry Pi camera was used to take frontal images of the embankment section. The model geometry and instrumentation layout are schematically shown in Figure 2.

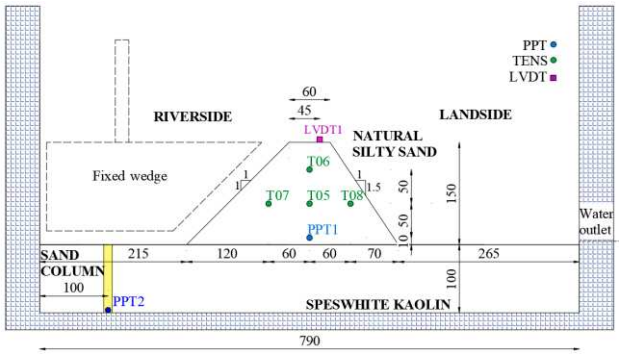

Figure 2. Schematic of the centrifuge model cross-section and instrumentation layout (dimensions are shown in mm, at the model scale).

Tensiometers used in the centrifuge test were manufactured by the National Research Facility for Infrastructure Sensing (NRFIS) of the University of Cambridge, following the low-cost manufacturing proposed by Jacobsz (2018). A porous ceramic filter, with an air entry value of 3 bar, was fitted to a MS54XX miniature pressure sensor from Measurement Specialties™ and the assembly was sealed with an epoxy resin. Before being installed within the embankment model, the tensiometers were accurately saturated and calibrated in a custom-built steel four-inlet manifold with Perspex walls, shown in Figure 3. Sealing was accomplished by using cable glands. The procedure described by Take and Bolton (2003) was followed for the saturation of the sensors.

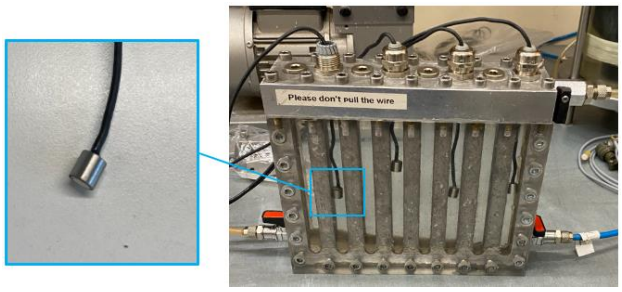

Figure 3. Picture of the steel manifold used for saturating tensiometers and a close-up view of the instrument.

3 TEST PROCEDURE

Once the model was embarked onto the swinging platform, it was gradually accelerated to 50 g over the time period t_1, as shown in Figure 4. The acceleration was then maintained at a constant level until the end of the test. Upon achieving the target angular speed, the model was allowed to reach self-

weight equilibrium for about 28 minutes (from t_1 = 926 s to t_2 = 2590 s). Subsequently, to study the hydro-mechanical response of the earthen structure to a simulated high-water event, the hydrometric level was increased from the control room. Water was allowed to flow inside the strongbox through a hole drilled in its back wall, in correspondence of the toe of the embankment on the riverside. Fluid level was controlled with a custom in-flight hydraulic load control system, consisting of an external standpipe with three holes, positioned at different elevations, respectively equal to 30, 60 and 90% of the post consolidation embankment height, H_{emb}, and acting as overflow outlets (Fig. 5). Each hole was connected to a solenoid valve through a pipe. Once a target water level was reached and kept constant for the time necessary to establish steady-state conditions, the hydraulic head was raised, by closing the corresponding solenoid valve and/or increasing the incoming flow rate.

River stage was monitored using the PPT2, along with an additional pore pressure transducer positioned at the base of the standpipe and visualised through the Perspex wall, by a frontal Raspberry Pi camera. A fixed wedge, schematically shown in Figure 2, was used to reduce the volume of water flowing inside the strongbox and to make the hydraulic load changes as quick as in reality.

As reported in Fig. 4, the hydraulic loading history was applied in three steps: the river stage was raised to the first target level of 0.2 H_{emb} and maintained constant up to the achievement of stationary seepage conditions (until t_3 = 3766 s); then the hydraulic head was further increased to 50% of the embankment height and kept at this level for about 10 minutes (until t_4 = 4316 s). Finally, a water level of 0.7 H_{emb} was imposed and, due to the progressive saturation of the embankment body and the consequent decrease in the effective soil shear strength, the failure of the landside slope occurred at t_5 = 4824 s.

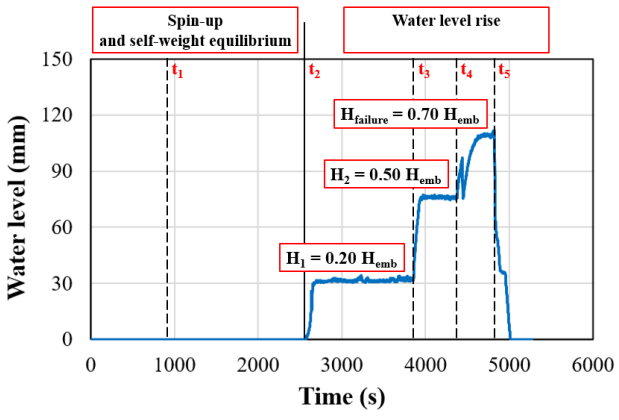

Figure 4. Centrifuge test phases and hydrograph imposed (time and hydraulic head at the model scale).

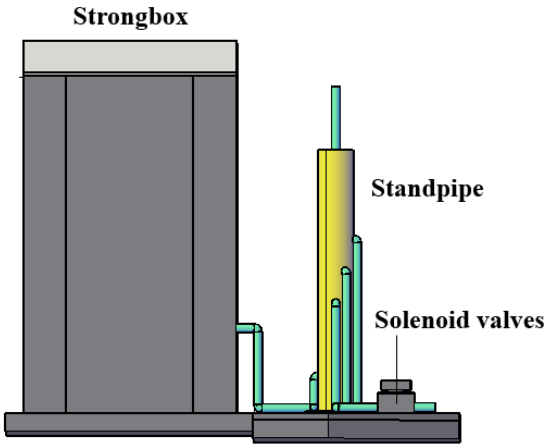

Figure 5. Lateral view of the in-flight hydraulic load control system.

4 EXPERIMENTAL OUTCOMES

The trend of vertical displacements over time of the embankment body, recorded by an LVDT located on the crest towards the landside, are shown in Figure 6; displacements are negative if downward. A progressive settlement of approximately 7 mm (0.35 m at prototype scale) was observed during the initial spin-up of the model and self-weight equilibrium phases, mainly due to the deformation of the foundation layer under the footprint of the embankment body, as visible in Figure 8a. A significant displacement occurred as a result of the increment of the centrifuge acceleration to 50 g, while minor settlements have been detected during the in-flight consolidation stage. An additional displacement of approximately 1.5 mm was recorded following the increase of the water level, up to the second target. Subsequently, once a steady-state flow regime was established in equilibrium with the 0.70 H_{emb} water level, the vertical displacements suddenly increased, reaching their maximum value at t_5, the time instant corresponding to the slope failure

Figure 7 shows the time history of the positive and negative pore water pressures (PWPs) measured during the test, by the sensors positioned in the embankment body at three different depths from the crown (sensor locations are shown in Fig. 2). All tensiometers recorded an initial suction between -2 and -7 kPa, which progressively tended to increase, during the spin-up of the model and the subsequent self-weight equilibrium stage, due to evapo-transpiration phenomena. Tensiometer T06 stopped working during the initial stage of the test.

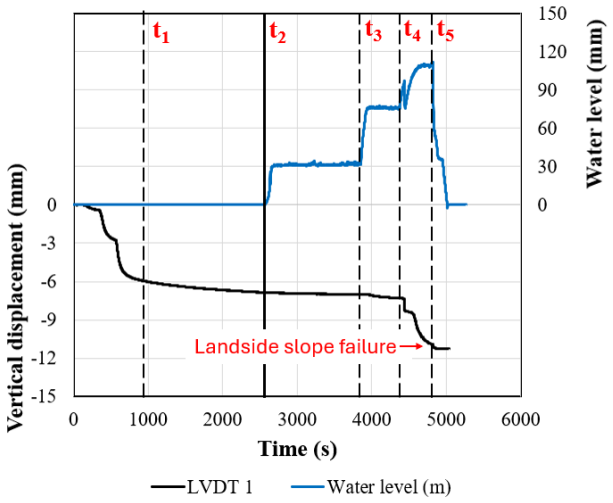

Figure 6. Time history of the vertical displacement of the embankment crest and the imposed hydrograph.

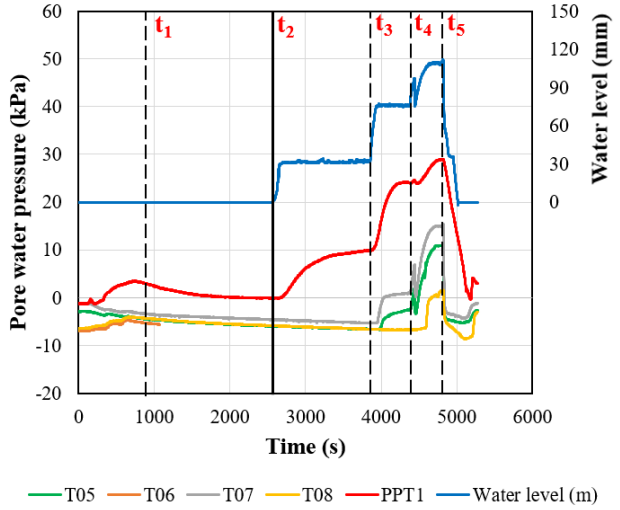

Figure 7. Pore water pressure trends recorded by the tensiometers and the PPT1 over time, along with the imposed hydrograph.

During the simulated high-water event, a groundwater seepage towards the landside occurred. The sensors installed closer to the riverside of the embankment instantly reflected water level changes, while tensiometers located along the vertical central alignment and on the landside were influenced by the advancement of the phreatic surface with a certain delay, as a function of the hydraulic and retention properties of the earthfill.

In particular, following the first hydraulic load, equal to 20% of the embankment height, a pore water pressure increase was recorded only by PPT1, positioned at an elevation of 10 mm above the ground level, while all the other tensiometers continued to detect negative pressure values, indicating that the wetting front was below their elevation. As the water head reached 50% of the embankment height, pressure values recorded by the tensiometers T05 and T07 started to increase, due to the progressive saturation of the surrounding soil, while the tensiometer T08, located towards the landward, remained in partially saturated conditions. Only the application of the third hydrometric level (0.70 H_{emb}) allowed for the saturation of the downstream slope, up to the elevation of tensiometer T08, which, shortly before the instant t_5, reached a positive pore pressure value. As soon as a steady-state flow regime, in equilibrium with the maximum hydrometric level applied was reached, all the sensors recorded peak values of pore water pressures, which were then followed by a sudden decrease, corresponding to the landside slope failure (Figure 8b) and the river level dropped.

The groundwater seepage phenomena occurring within the embankment body can be thoroughly understood by observing the pore water pressure isochrones along the horizontal alignment defined by tensiometers T07, T05, and T08, at significant time intervals (i.e., t_1, t_2, t_3, t_4, and t_5), shown in Figure 9. The x-axis represents the horizontal distance measured from the embankment foot on the riverside to the tensiometers T07, T05 and T08.

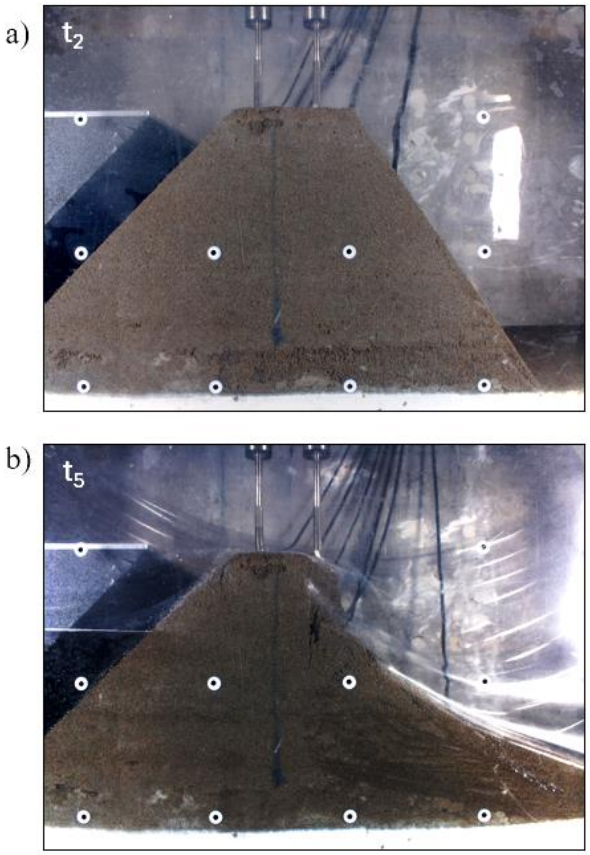

Figure 8. Pictures of the river embankment model: a) at the end of the in-flight consolidation (t_2 = 2590 s); b) following the collapse of the landside slope (t_5 = 4824 s).

At the end of the in-flight consolidation stage (t_2) and following the first water level imposed (t_3), the embankment body resulted still unsaturated up to the elevation of the three highlighted tensiometers. At t_4, only T07, located closer to the riverside, measured a positive pore water pressure value, while the other sensors continued to register suctions, although a significant increase in pore pressures can be noted, confirming the advancement of the wetting front towards the landside. Finally, at t_5, all tensiometers measured positive pore water pressures. The seepage process established in the embankment body led to the nullification of the suction contribution to the shear strength resistance, triggering the collapse of the landside slope.

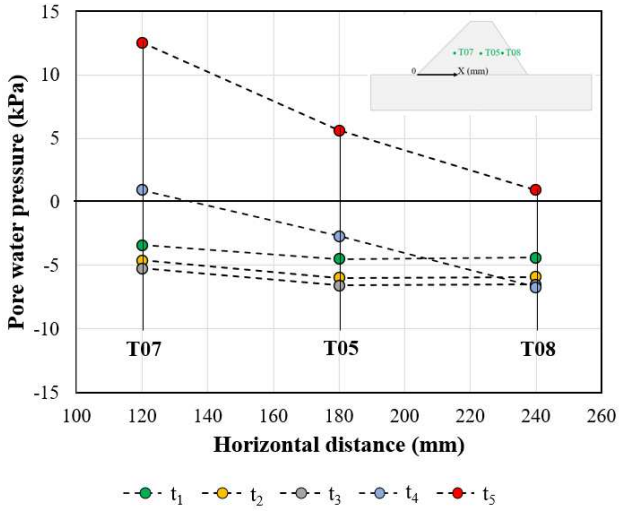

Figure. 9 Isochrones of pore water pressures at significant time-steps along the horizontal alignment given by T07-T05-T08.

5 CONCLUDING REMARKS

This paper illustrated the experimental setup and preliminary findings of a centrifuge test conducted on a natural silty sand river embankment model, subjected to a simulated high-water event. The embankment body was instrumented with in-house built miniaturized tensiometers and PPTs, to monitor pore pressure and suction distribution changes, as a function of the increasing water level. Settlements were observed through an LVDT, installed on the crest. The analysis of the monitoring data showed that, in the absence of flood protection measures, such as cut-off barriers, drains, and reinforcement layers, if the earth structure is characterized by steep slopes, the instability of the landside slope might occur, leading to catastrophic consequences for the surrounding area.

6 ACKNOWLEDGMENTS

The financial support provided by the European Union's H2020 Research and Innovation GEOLAB programme, grant agreement No. 101006512, is gratefully acknowledged. Appreciation is also extended to the technicians of the Schofield Centre and the NRFIS from the University of Cambridge for their assistance, and to Prof. Gopal Madabhushi for his hospitality.

7 REFERENCES

Alcamo, J., M. Flörke, and M. Märker. (2007). Future long-term changes in global water resources driven by socio-economic and climatic changes. Hydrological Sciences Journal, 52 (2): 247–275.

Cargill, K. W., and H. Ko. (1983). Centrifugal Modeling of Transient Water Flow. *J. Geotech. Engrg*., 109 (4): 536–555.

Garnier, J., C. Gaudin, S. M. Springman, P. J. Culligan, D. Goodings, D. Konig, B. Kutter, R. Phillips, M. F. Randolph, and L. Thorel. (2007). Catalogue of scaling laws and similitude questions in geotechnical centrifuge modelling. *International Journal of Physical Modelling in Geotechnics*, 7 (3): 01–23.

Jacobsz, S. W. (2018). Low cost tensiometers for geotechnical applications. *Proc. of the 9th Int. Conf. on Physical Modelling in Geotechnics*, Taylor and Francis Group, CRC Press, London

Madabhushi, G. (2015). Centrifuge Modelling for Civil Engineers. CRC Press, London, UK.

Rocchi, I., C. G. Gragnano, L. Govoni, M. Bittelli, and G. Gottardi. (2020). Assessing the performance of a versatile and affordable geotechnical monitoring system for river embankments. *Physics and Chemistry of the Earth*, 117: 102872. https://doi.org/10.1016/j.pce.2020.102872

Singh, J., K. Horikoshi, Y. Mochida, and A. Takahashi. (2019). Centrifugal tests on minimization of flood-induced deformation of levees by steel drainage pipes. *Soils and Foundations*, 59 (2): 367–379. https://doi.org/10.1016/j.sandf.2018.12.008

Take, W. A., and M. D. Bolton. (2003). Tensiometer saturation and the reliable measurement of soil suction. *Géotechnique*, 53 (2): 159–172. https://doi.org/10.1680/geot.2003.53.2.159

Van, M.A., Rosenbrand, E., Tourment, R., Smith, P. and Zwanenburg, C. (2022). Failure paths for levees." ISSMGE – Technical Committee TC201 'Geotechnical aspects of dikes and levees,' 134. https://doi.org/10.53243/R0006

Ventini, R., E. Dodaro, D. Giretti, M. Pirone, F. Zarattini, C. G. Gragnano, V. Fioravante, F. Gabrieli, G. Gottardi, and C. Mancuso. (2023). Analysis of transient seepage through a river embankment by means of centrifuge modelling. *Proc. of the 8th Int. Conf. on Unsaturated Soils*, Milos, Greece. https://doi.org/10.1051/e3sconf/202338212008

Viggiani, G. (1992). *Small strain stiffness of fine grained soils*, Doctoral dissertation, City University, London.